Brain Research 1817 (2023) 148495

Contents lists available at ScienceDirect

Brain Research

journal homepage: www.elsevier.com/locate/brainres

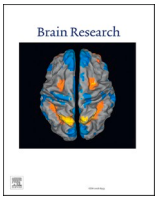

Dynamic changes of oligodendrogenesis in neonatal rats with hypoxic-ischemic white matter injury

Qing Lin [a,b,1], Ling Lin [c,1], Li Li [d,1], Yu-fen Zheng [a], Ding-wang Hu [a,b,*], Geng Zhang [a,b,*]

[a] Fujian Provincial Key Laboratory of Brain Aging and Neurodegenerative Diseases, Fujian Medical University, Fuzhou, China
[b] Laboratory of Clinical Applied Anatomy, Department of Human Anatomy, School of Basic Medical Sciences, Fujian Medical University, Fuzhou, China
[c] Public Technology Service Center, Fujian Medical University, Fuzhou, China
[d] Assisted Reproduction Centre, Obstetrics and Gynecology Department, 900TH Hospital of Joint Logistics Support Force, Fuzhou, China

ARTICLE INFO

Keywords:
Oligodendrogenesis
Hypoxia–ischemia
White matter injury
Neonatal rats

ABSTRACT

Background: White matter injury (WMI) is an important type of preterm brain injury, which may result in severe neurological sequelae and lack of effective treatments. It is ascertained that selective vulnerability of oligodendrocytes is closely related to the WMI in preterm infants. But the alteration of the endogenous oligodendrogenesis over long time after hypoxic-ischemic WMI is still not clearly elucidated.
Methods: We adopted an animal model of hypoxic-ischemic WMI in 3-day-old neonatal Sprague-Dawley rats. Immunofluorescence staining and western blotting were used to detect dynamic changes of oligodendrogenesis in the white matter region on postoperative day (POD) 1, 3, 7, 14, 28, 56 and 84.
Results: In the sham group, the oligodendrocyte lineage in the white matter reached a developmental peak from POD 3 to 14. The proliferation and development of oligodendrocyte precursor cells (OPCs) occurred primarily within POD 14. The number of mature oligodendrocytes showed an upward trend and a dynamic change in proliferation over time. While in the WMI group, the oligodendrocyte lineage was upregulated on POD1 and 3 but downregulated on POD 7 and 14. The proliferation of OPCs increased on POD 1 and decreased on POD 3 and 7, with the total number of OPCs significantly reduced from POD 3 to 14. The number of mature oligodendrocytes decreased from POD 3 to 28, and return to the level of the sham group on POD 56 and 84, whereas the MBP expression was still significantly downregulated on POD 56 and 84.
Conclusions: Hypoxia-ischemia can have a long-term dynamic effect on the endogenous oligodendrogenesis of neonatal rat brain white matter. The proliferation of OPCs was promoted on POD 1 but inhibited from POD 3 to 14, which may be an early intervention target to improve oligodendrogenesis. The number of mature oligodendrocytes recover to the normal on POD 56 and 84 but the myelination is still blocked, which suggests it is essential to promote the maturation of oligodendrocyte and its function recovery at the same time within POD 28. Such efforts will provide the opportunity to test new interventions in pre-clinical studies for their promising clinical application.

1. Introduction

White matter injury (WMI) is an important type of preterm brain injury, especially in very low birth weight infants (Liu et al., 2013), which may result in severe neurological sequelae, including visual disorder, behavior and cognitive impairment (Back, 2017; Marlow et al., 2005), and even cerebral palsy (Derrick et al., 2007).Currently, there is a lack of effective treatment for WMI. Therefore, effective prevention and treatment of this disease has become an urgent problem and a challenge for neonatal medicine worldwide.

WMI is accompanied by dysmyelination, axonal injury, and oligodendroglial loss and has been confirmed to be the key reason of cerebral

Abbreviations: CC, corpus callosum; MBP, myelin basic protein; OL, oligodendrocyte; Olig2, OL transcription factor 2; OPCs, oligodendrocyte precursor cells; PBS, phosphate buffered saline; PDGFRα, platelet-derived growth factor receptor α; POD, postoperative day; PVDF, polyvinylidene fluoride; ROS, reactive oxygen species; SD, standard deviation; WMI, white matter injury.

* Corresponding authors at: No.1 Xuefu North Road, University Town, Fuzhou, Fujian Province, China.
E-mail addresses: hdw2014@sina.com (D.-w. Hu), zhg9355@126.com (G. Zhang).

[1] These authors contributed equally to this work.

https://doi.org/10.1016/j.brainres.2023.148495
Received 30 April 2023; Received in revised form 18 July 2023; Accepted 19 July 2023
Available online 20 July 2023

palsy in survivors. Lots of studies have proved that the selective vulnerability of oligodendrocyte precursor cells (OPCs) is strongly associated with WMI in the preterm(Liu et al., 2013; Back et al., 2002; Cai et al., 2018). The gestational ages of preterm infants ranging from 23 to 32 weeks were a predilection time period for white matter lesions wherein OPCs accounted for a large proportion at this phase, and they were more sensitive to hypoxia–ischemia than neurons (Liu et al., 2013). OPCs tend to be damaged and lost during hypoxia–ischemia(Volpe et al., 2011), leading to a reduction in the number and dysfunction of mature oligodendrocyte (OLs) that migrate and differentiate from OPCs, eventually leading to myelination disorder in the white matter region. Thus, the vulnerability of OPCs to hypoxia–ischemia is essential for the pathogenesis and progression of WMI in preterm infants.

Oligodendrogenesis refers to the processes that OPCs differentiate into mature oligodendrocytes, which are then able to enwrap and myelinate axons. Myelination is a highly coordinated process in which OPCs proliferate and migrate towards exposed axons (Franklin and Blakemore, 2013). OPCs then differentiate into premyelin OLs and extend multiple processes to contact axons, but myelination is yet to be initiated. When primary axon-derived OLs differentiation inhibitors are withdrawn (Almeida, 2018), pre-myelinated OLs contract their secondary and tertiary processes, and the myelin membrane is wrapped around the tip of the primary processes. These myelin membranes wrap axons multiple times and are subsequently reduced through the cytoplasm and exoplasm to form dense myelin (Fancy et al., 2010). It has been elucidated that the foxO1-P27kIP1 pathway promoted oligodendrogenesis in neonatal rats with hypoxic WMI (Jablonska et al., 2012). But currently, there is no comprehensive literature on whether endogenous oligodendrogenesis changes dynamically over a long time after hypoxic-ischemic WMI. The research on this problem will help to provide a new way for clinical treatment of WMI in premature infants by targeting oligodendrogenesis. Our study aimed to adopt an animal model of hypoxic-ischemic WMI in neonatal rats and investigate the dynamic changes of oligodendrogenesis in the white matter region over time by using morphological and molecular biology techniques, which could further contribute to a better elucidation of the pathogenesis of hypoxic-ischemic WMI that may provide an adequate theoretical foundation for the clinical treatment of premature WMI with oligodendrogenesis as the target.

2. Materials and methods

2.1. Animal

A total of 88 neonatal (3-d-old, 8–11 g) Sprague-Dawley rats were provided by the Experimental Animal Center of Fujian Medical University. The neonatal rats were grown with mother rats and maintained on a 12-/12-hour light/dark cycle with access to food and water ad libitum. All experimental procedures were approved by the Animal Care and Use Committee of Fujian Medical University [Animal License Number: SYXK (Min) 2016–0007], and performed in accordance with the relevant guidelines and regulations. Maximal care was taken to reduce the number of animals employed and minimize any pain and distress during the study.

2.2. WMI rat model

Animals were randomly assigned to the sham and WMI groups (n = 44 neonatal rats per group, maintaining a male to female ratio of 1:1 in each group). The WMI rat model (bilateral common carotid artery electrocoagulation combined with hypoxia) was established as previously described (Hu et al., 2022; Wang et al., 2016). Three-day-old neonatal rats were anesthetized by inhalation of 2% isoflurane in oxygen flow using a small animal anaesthesia machine (Shenzhen RWD Life Science Co. Ltd, Shenzhen, China). The skin of the neck was exposed and disinfected with 75% alcohol. A median incision of approximately 5 mm was made, and the bilateral common carotid arteries were cut off permanently by electrocoagulation in the WMI group. The skin incision was sutured, and the rats were placed at 37 °C for 10 min until their body temperature and activity returned to normal. After returning to the cage for 2 h, rats were again exposed to 8% O_2/92 % N_2 at 37 °C for 30 min. In the sham group, the bilateral common carotid arteries were only separated without electrocoagulation, and the rats were separated from the mother rat and exposed to ambient air for 30 min.

2.3. Immunofluorescence staining

Rats were deeply anesthetized with isoflurane on postoperative day (POD) 1, 3, 7, 14, 28, 56 and 84, and transcardially perfused with 0.01 M phosphate buffered saline (PBS) followed by 4% paraformaldehyde (Lin et al., 2023). Brains were dissected and then cryoprotected with 30% sucrose in 0.01 M PBS at 4 °C. Coronal brain sections (14 μm thick) were collected using a cryostat microtome (Leica CM1950, Germany). Collected sections were washed with 0.01 M PBS for three times, blocked in Immunol Staining Blocking Buffer (Beyotime, P0102, Shanghai, China) for 1 h at room temperature, followed by incubation in the following primary antibodies for 48 h at 4 °C: Myelin Basic Protein (D8X4Q) XP® Rabbit mAb (1:500, Cell Signaling Technology, 78896, Massachusetts, USA), Anti-activated caspase-3 (1:200, Proteintech, 19677–1-AP, USA), Anti-Olig2 antibody (1:500, Sigma-Aldrich, MABN50, Saint Louis, USA), Anti-Ki67 antibody (1:500, abcam, ab16667, Cambridge, England), PDGFR-α (C-9) (1:200, Santa Cruz Biotechnology, sc-398206, Santa Cruz, California), Anti-APC antibody (1:400, abcam, ab16974, Cambridge, England). Sections were then rinsed three times in 0.01 M PBS and incubated with the following second antibodies: Donkey Anti-Rabbit IgG H&L Alexa-555 (1:500, abcam, ab150062, Cambridge, England), Biotinylated Goat Anti-Rabbit IgG antibody (1:200, Vector Laboratories, BA-1000, Burlingame, USA), Biotinylated Goat Anti-Mouse IgG antibody (1:200,Vector Laboratories, BA-9200, Burlingame, USA), PierceTM Avidin Fluorescein Conjugated (1:500, Thermo, 21221, Massachusetts, USA). Nuclei were stained with DAPI (1:1000, Beyotime, C1002, Shanghai, China). After rinsing with 0.01 M PBS, sections were mounted on slides using antifade mounting medium (Beyotime, P0126, Shanghai, China), and visualized under a confocal laser scanning microscope (Leica TCS SP8, Germany).

2.4. Quantification of immunopositive cells

The quantitative method for immunopositive cells has been improved based on the previous protocols (Flygt et al., 2013). Rat brains of both sham and WMI groups were dissected on POD 1, 3, 7, 14, 28, 56 and 84. Consecutive coronal brain sections (14 μm thick) were collected using a cryostat microtome. Three nonadjacent brain slices were selected from each animal (Fig. 1). All animals were selected from the same three coronal sections for immunofluorescence staining. All immunofluorescence images were captured by an investigator who was blinded to the experimental group assignment. The parameters for image acquisition were identical for each brain slice in the same region of interest. And a total of 10 microscopic fields for each animal (Fig. 1) were acquired with a 40X objective from the corpus callosum (CC) for

Fig. 1. Diagrammatic representation of coronal sections of rat brain. Microscopic fields acquired from the corpus callosum for quantification are represented by the red boxes. (For interpretation of the references to colour in this figure legend, the reader is referred to the web version of this article.)

quantification. Immunopositive cells were counted via Image J software in an unbiased manner by an observer who was blinded to the experimental group assignment. Results were presented as positive cells density (cells/mm^2).

2.5. DHE staining

The levels of reactive oxygen species (ROS) production in the brain tissues were assessed by dihydroethidium (DHE) staining, as previously described (Santana-Garrido et al., 2020). Briefly, 14 μm thick frozen brain sections were prepared and incubated with 5 mM DHE (MedChemExpress, HY-D0079) for 30 min at 37 °C in a humidified chamber. After staining with DAPI, the immunofluorescence images were captured by a confocal laser scanning microscope (Leica TCS SP8, Germany) with the same parameters (Objective: 20×; ZOOM: 2.0; Excitation wavelength: 552 nm; Emission wavelength: 565–620 nm; Pinhole size: 1.00AU; Laser power: 2.05%; Gain: 643; Offset: −2). Ten fields were selected from each animal (Fig. 1), and the fluorescence intensity for DHE was determined directly using confocal laser scanning microscope.

2.6. Western blotting

Western blotting was performed to detect myelin basic protein (MBP) expression in white matter on POD 14, 28, 56 and 84 according to our previously established protocols (Lin et al., 2023). Tissue samples of the CC were dissected and lysed in ice-cold radioimmunoprecipitation assay buffer. Equal amounts of protein (60 μg) were loaded onto a 12% sodium dodecyl sulfate–polyacrylamide gel electrophoresis gel. After electrophoresis and transfer to polyvinylidene fluoride (PVDF) membrane (MerckMillipore), the blots were cut in order to assure that normalization were performed with β-actin and MBP on the same membrane to account for variations in loading. Then the membranes were blocked with 5% skim milk at room temperature for 2 h and then incubated with Myelin Basic protein (D8X4Q) XP® rabbit mAb (1:1000, Cell Signaling Technology, 78896, Massachusetts, USA) or rabbit anti-beta actin antibody (1:2000, BBI, D110001-0100, China) overnight at 4 °C. After washing in TBST three times for 10 min each, the PVDF membrane was incubated with goat anti-rabbit IgG/HRP antibody (1:1000, Bioss, bs-0295G-HRP, Beijing, China) for 2 h at room temperature. After rinsing with TBST, the PVDF membranes were visualized by enhanced chemiluminescence (Meilunbio) using the Chemiluminescence Imaging System (Amersham Imager 680, USA).

2.7. Statistical analysis

All data are presented as mean ± standard deviation (SD). Data were analyzed using GraphPad Prism 8 software (GraphPad Software, CA, USA). Statistical differences between groups were detected using unpaired two-tailed Student's *t* test or two-way ANOVA followed by Tukey's multiple comparison test. Differences were considered statistically significant at $P < 0.05$. P values are annotated in the figures.

3. Results

3.1. Dysmyelination of white matter in rats after hypoxia–ischemia

To observe the changes in the myelin sheath in white matter after hypoxia–ischemia, we used western blotting and immunofluorescence staining to observe changes in MBP expression. We found that MBP was not detected in the CC of the sham and WMI group on POD 1, 3 and 7 (data was not shown). The fluorescence intensity of MBP in the CC of the WMI group was significantly lower than that in the sham group on POD 14 and 28 (Fig. 2A-2D). Meanwhile, western blotting showed that the expression of MBP in the WMI group was significantly downregulated compared to that in the sham group on POD 14 and 28 ($p < 0.01$; Fig. 2E-2F). These results imply that WMI occurs after hypoxia–ischemia in neonatal rats.

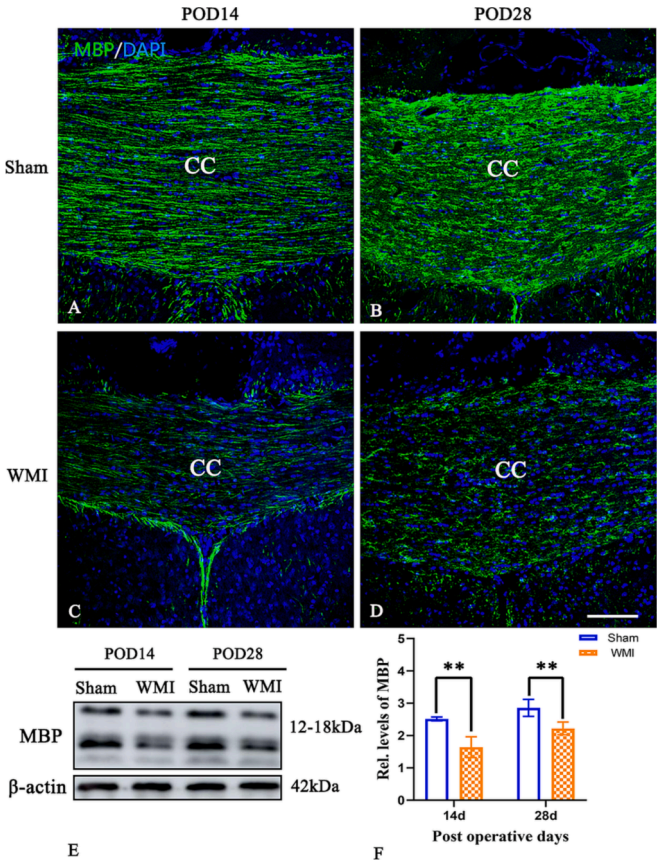

Fig. 2. The effect of hypoxia–ischemia on myelin basic protein (MBP) level in brain on postoperative day 14 and 28. **(A-D)** Representative images of the immunolabeling for MBP (green) and DAPI (blue) in the cerebral white matter (corpus callosum [CC]). **(E-F)** Western blot images showed MBP level clearly reduced in WMI group compared with sham group on POD 14 and 28. Detected western blot intensities for MBP were normalized to corresponding β-actin band intensities. All data represent the mean ± SD, $^{*}p < 0.05$, $^{**}p < 0.01$, unpaired *t* test, n = 4 per group. Scale bar, 100 μm. (For interpretation of the references to colour in this figure legend, the reader is referred to the web version of this article.)

3.2. Increase of oxidative stress and apoptotic oligodendrocytes after hypoxia–ischemia

Oxidative stress levels of the white matter (corpus callosum) after hypoxia–ischemia were measured by DHE staining. As shown in Fig. 3, the DHE immunofluorescence intensity were markedly enhanced in the WMI group compared to the sham group on POD 1, 3, 7, 14 and 28 ($p < 0.001$), which indicated the increase in generation and distribution of reactive oxygen species (ROS) in brain tissues after hypoxia–ischemia. Our results showed no significant difference of the DHE fluorescent density between the two groups on POD 56 and 84 ($p > 0.05$).

Increased oxidative stress may lead to cell damage through lipid peroxidation pathway. In present study, hypoxia ischemia-induced apoptosis of oligodendrocytes was evaluated by Olig2 (oligodendrocyte transcription factor 2) and activated apoptotic marker caspase-3 double-labeling. The caspase-3-immuno-positive cells were co-localized with Olig2 (marker for oligodendrocytes at all stages of development) in the corpus callosum (Fig. 4, arrows). We counted the caspase-3 and Olig2- positive cells in the corpus callosum in all rats, and found the number of apoptotic oligodendrocytes significantly increased in the WMI group on POD 3, 7 and 14 (Fig. 4, $p < 0.001$), indicating the

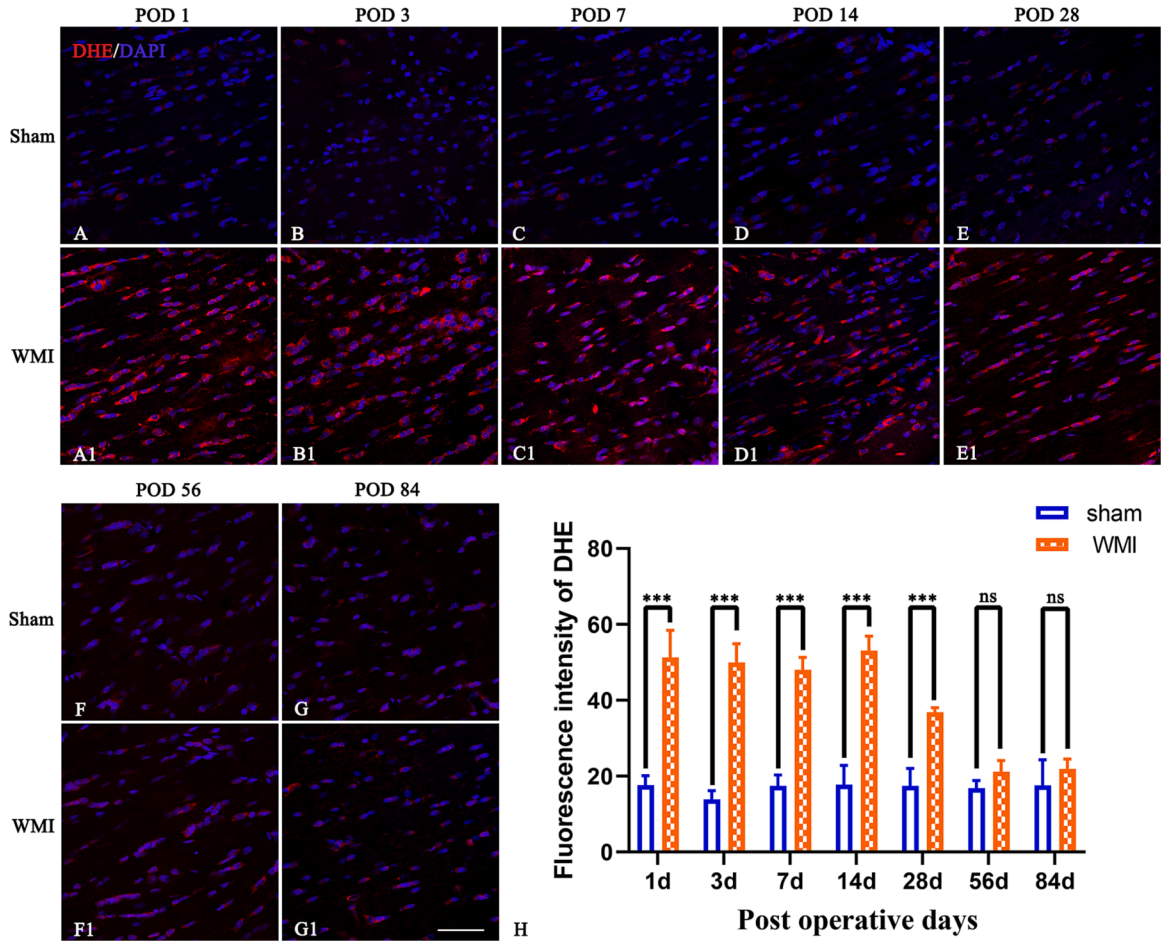

Fig. 3. Oxidative stress increased in the corpus callosum after hypoxia–ischemia. **(A–G, A1-G1)** Representative confocal images for staining with DHE (red) and DAPI (blue) in the corpus callosum. **(H)** Quantitative analysis of the DHE immunofluorescence intensity in both groups at different time points. The fluorescent density of DHE was significantly increased in the WMI group on POD 1, 3, 7, 14 and 28. Data are presented as mean ± SD, ***$p < 0.001$, n = 4 per group. Scale bar, 50 μm. (For interpretation of the references to colour in this figure legend, the reader is referred to the web version of this article.)

involvement of caspase-3-mediated apoptosis in the death of OLs. However, there was no statistical difference of the apoptotic OLs between the two groups on POD 1, 28, 56 and 84 ($p > 0.05$).

3.3. The changes of OL lineage in white matter over time

OL transcription factor 2 (Olig2), which is expressed in the nucleus, was used to label all OL-lineage cells. Ki67 is a cell proliferation marker expressed in the nucleus, and changes in the density of $Olig2^+$-, $Ki67^+$-, and $DAPI^+$ positive cells can reflect changes in proliferating OL-lineage cells. To observe the expression of the OL lineage in the WMI and sham groups, triple immunofluorescence staining for Olig2, Ki67, and DAPI was performed on brain tissues (Fig. 5A-5F, 5A1-5F1 showing representing images). $Olig2^+$ OL lineage cells were distributed throughout the brain, especially in the white matter. Positive cells were counted in the CC region.

In the sham group, the number of OL lineages gradually increased and peaked on POD 14, then began to decline, and became stable on POD 28, which is comparable with that on POD 3. Additionally, the number of OL lineages in the WMI group peaked on POD 3 and remained at this level. By comparing the total number of cells in the two groups at the same time point, it was found that the increase in the number of OL lineages in the WMI group was significantly higher than that in the sham group on POD 1 and 3 ($p < 0.01$), but lower than that in the sham group on POD 7 and 14 ($p < 0.01$). There was no statistical difference between the groups on POD 28, 56 and 84 ($p > 0.05$) (Fig. 5G).

The change tendency of the proliferating OL lineage was generally consistent over time in the WMI and sham groups, presenting a decline first and then a gradual uptrend followed by a further downtrend, and finally stabilizing. On POD 1, the number of proliferating OLs in the WMI group was higher than that in the sham group ($p < 0.05$), but on POD 3 and 7, it was significantly lower than that in the sham group ($p < 0.01$). On POD 7, the number of proliferating OLs in both groups reached a maximum value. There was a small increase followed by a decrease on POD 28 in the WMI group, whereas there was a small increase followed by a decrease on POD 56 in the sham group. And there was no statistical difference between the groups on POD 14, 56 and 84 ($p > 0.05$) (Fig. 5H).

3.4. The changes of OPCs in white matter over time

The OL lineages include OPCs, immature OLs, and mature OLs. Changes in the number and proliferation of OPCs may alter the total number of OL lineages. Therefore, fluorescence triple-labeling with PDGFRα (platelet-derived growth factor receptor α), Ki67, and DAPI was used to observe changes in the expression of OPCs in the WMI and sham groups. Among them were OPCs (PDGFRα + -labeled), proliferating OPCs (PDGFRα + Ki67 + DAPI + -labeled), and non-proliferating OPCs (PDGFRα + Ki67-DAPI + -labeled) (Fig. 6A-6F, 6A1-6F1).

The statistical results of PDGFRα-positive cells showed that the total number of OPCs in the sham group began to increase after surgery, reached a peak on POD 7, then decreased, and was lowest on POD 14

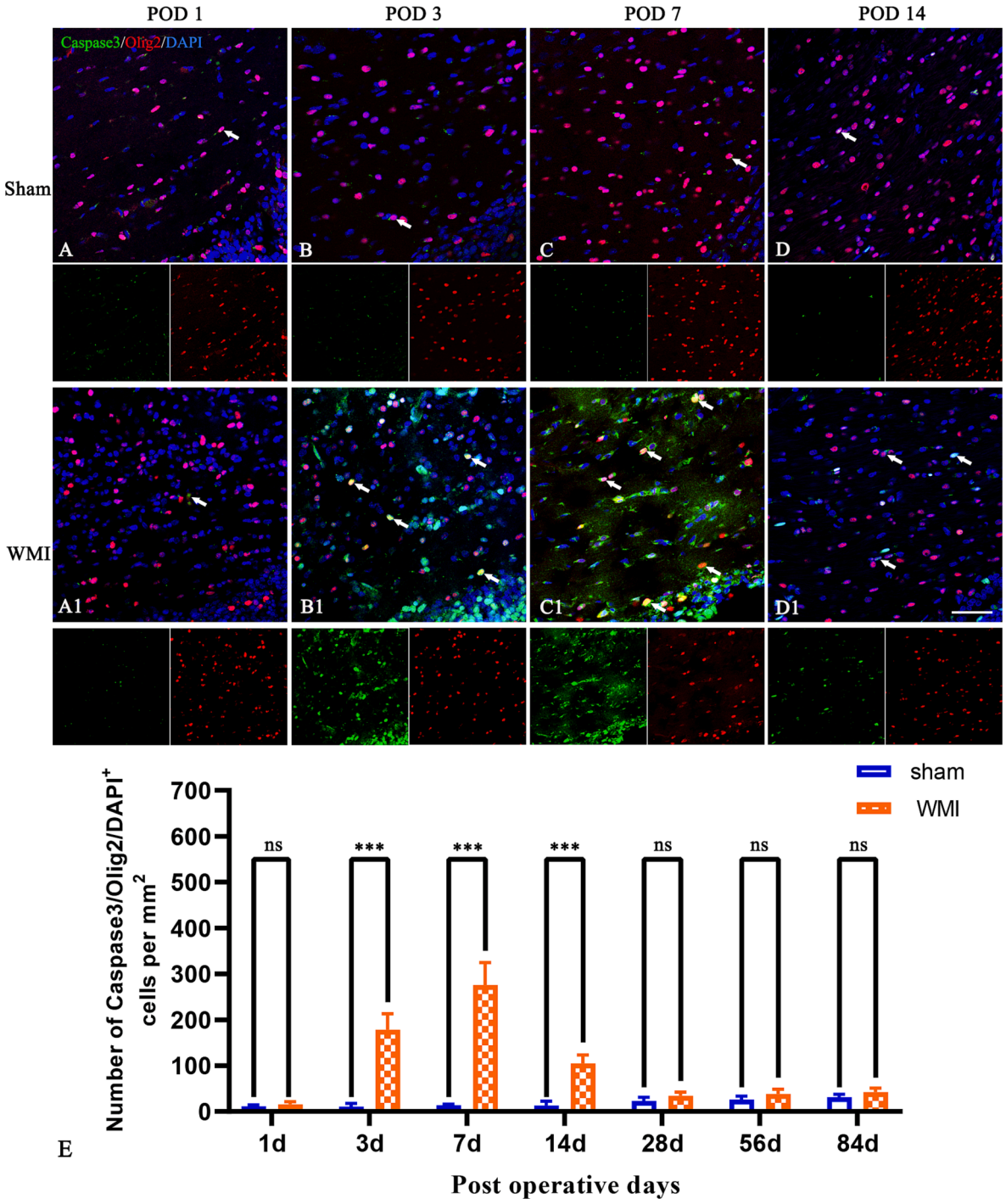

Fig. 4. OL apoptosis occured in the corpus callosum after hypoxia–ischemia. **(A–D, A1-D1)** Apoptotic OLs were evaluated with double staining for Olig2 (OLs; red), activated caspase-3 (green), and the nuclear marker DAPI (blue). Olig2 and activated caspase-3 co-labeling is indicated by white arrows. Apoptotic OLs were rare in sham group rats **(A-D)**. Numerous apoptotic OLs were observed on POD 3, 7 and 14 in WMI group **(B1-D1). (E)** Counts of the OL apoptosis in corpus callosum was evaluated on sections. Data are presented as mean ± SD, $^{**}p < 0.001$, n = 4 per group. Scale bar, 50 μm. (For interpretation of the references to colour in this figure legend, the reader is referred to the web version of this article.)

and remained at this level thereafter. The total number of OPCs in the WMI group reached the maximum on POD 1, then decreased, and rose on POD 7, but it did not reach the level on POD 1, and continued to decline and remained at a low level on POD 14 (Fig. 6G). Comparing the total number of cells between the two groups at the same time point, we found that the total number of OPCs in the WMI group was significantly higher than that in the sham group on POD 1 ($p < 0.001$), but less than that in the sham group on POD 3 and 7 ($p < 0.0001$). There was no significant difference between the two groups on POD 14, 28, 56 and 84 (Fig. 6G).

The statistical results of $PDGFR\alpha^{+}Ki67^{+}DAPI^{+}$ cells showed that in the sham group, some OPCs were proliferating on POD 1, and the number of proliferating cells peaked on POD 7, then began to decrease, reached the lowest on POD 14, and maintained a low level thereafter. The proliferation trend of OPCs in the WMI group was consistent with that of the total number of OPCs. Comparing the number of proliferating

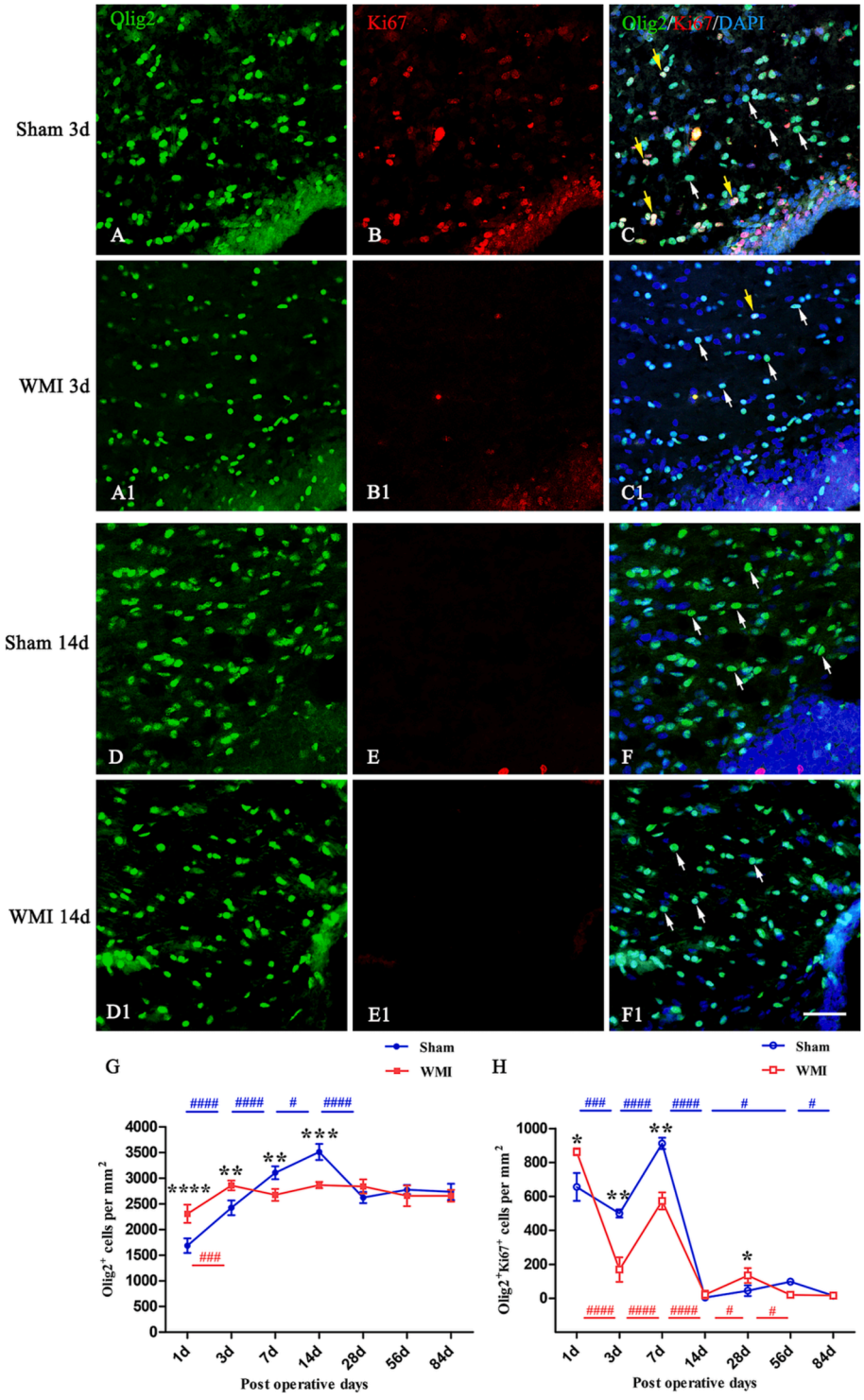

Fig. 5. The effect of hypoxia–ischemia on the total number and proliferation of oligodendrocyte (OL) lineages in white matter. **(A-F) and (A1-F1)** Representative images of the immunolabeling for OL transcription factor 2 (Olig2) (green), Ki67 (red) and DAPI (blue) in the cerebral white matter (corpus callosum [CC]) on postoperative day (POD) 3 and 14. The representative Olig2/DAPI-positive cells (white arrow) show the OLs; the representative Olig2/Ki67/DAPI-positive cells (yellow arrow) show the proliferation of OLs. **(G-H)** The chart of changing trends in the total number of OL lineages and proliferative OL lineages in white matter (CC) over time. *Indicates a statistical difference between the sham group and the WMI group at the same postoperative time point ($^{*}p < 0.05$, $^{**}p < 0.01$, $^{***}p < 0.001$, $^{****}p < 0.0001$); $^{\#}$ indicates that the same group has statistical differences at different postoperative time points ($^{\#}p < 0.05$, $^{\#\#\#}p < 0.001$, $^{\#\#\#\#}p < 0.0001$). All data represent the mean ± SD, two-way ANOVA with Tukey's multiple comparison test, n = 4 per group. Scale bar, 50 μm. (For interpretation of the references to colour in this figure legend, the reader is referred to the web version of this article.)

OPCs between the two groups at the same time point, it was found that the proliferation of OPCs in the WMI group was significantly higher than that in the sham group on POD 1 ($p < 0.05$), but it was less than that in the sham group on POD 3 and 7 ($p < 0.05$). There was no statistically significant difference between the two groups on POD 14 (Fig. 6H). These results suggested that the difference in the total number of OPCs between the two groups was caused by the difference in the proliferation of OPCs.

3.5. The changes of mature OL in white matter over time

OPCs can differentiate into mature OLs, and APC (a mature OLs marker) is mainly expressed in the cell bodies of mature OLs. To observe the proliferation of mature OLs after surgery, we used APC, Ki67, and DAPI for triple immunofluorescence staining. Mature OLs ($APC^{+}DAPI^{+}$-labeled) and newborn mature OLs ($APC^{+}Ki67^{+}DAPI^{+}$-labeled) are depicted in Fig. 7A-7F, and 7A1-7F1 (representing images on POD 3 and 14).

The statistical results of $APC^{+}DAPI^{+}$ cells showed that the total

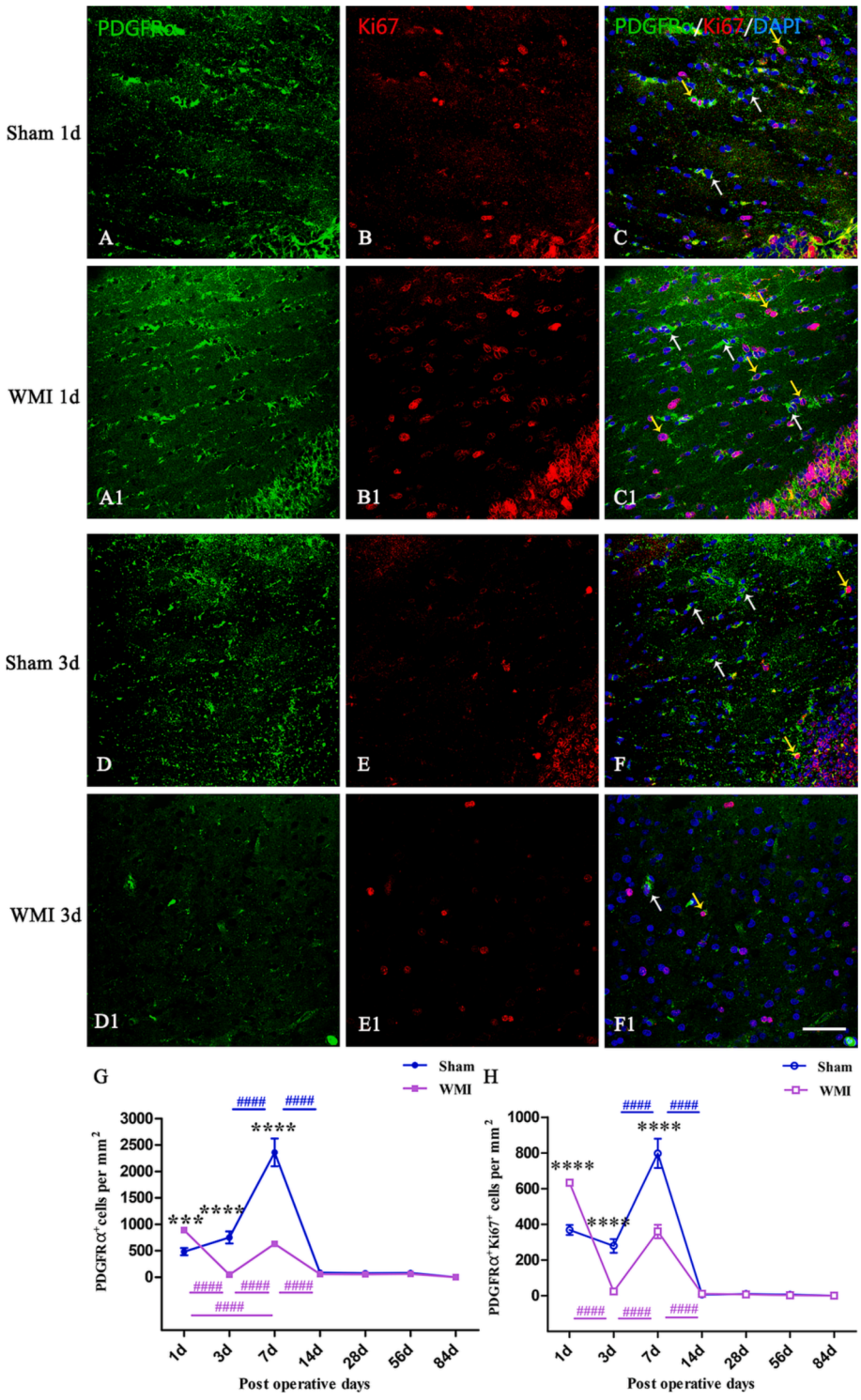

Fig. 6. The effect of hypoxia–ischemia on the total number and proliferation of oligodendrocyte precursor cells (OPCs) in white matter. **(A-F) and (A1-F1)** Representative images of the immunolabeling for PDGFRα (green), Ki67 (red) and DAPI (blue) in the cerebral white matter (corpus callosum [CC]) on postoperative day (POD) 1 and 3. The representative PDGFRα/DAPI-positive cells (white arrow) show the OPCs; the representative PDGFRα/Ki67/DAPI-positive cells (yellow arrow) show the proliferation of OPCs. **(G-H)** The chart of changing trends in the total number of OPCs and proliferative OPCs in white matter (CC) over time. *Indicates a statistical difference between the sham group and the WMI group at the same postoperative time point ($^{***}p < 0.001$, $^{****}p < 0.0001$); $^{\#}$ indicates that the same group has statistical differences at different postoperative time points ($^{\#\#\#\#}p < 0.0001$). All data represent the mean ± SD, two-way ANOVA with Tukey's multiple comparison test, n = 4 per group. Scale bar, 50 μm. (For interpretation of the references to colour in this figure legend, the reader is referred to the web version of this article.)

number of mature OLs in the sham and WMI groups had a consistent trend, reached a small peak on POD 7, and then slightly decreased on POD 14, but the number was higher than that on POD 1, which continued to increase on POD 28, and then peaked on POD 84. However, the total number of mature OLs in the WMI group was less than that in the sham group on POD 3, 7, 14, and 28 ($p < 0.05$; Fig. 7G).

Statistics of $APC^{+}Ki67^{+}DAPI^{+}$ cells showed that the proliferation of mature OLs in the sham group was most obvious on POD 7, followed by POD 3 and 28. However, the proliferation of mature OLs in the WMI group was lower and there was no significant change at any time point. Within POD 28, the proliferation of mature OLs in the WMI group was lower than that in the sham group ($p < 0.05$; Fig. 7H).

3.6. The expression of myelin basic protein decreased on POD 56 and 84

From the change trend of the mature OLs in the white matter over time, we found that the total number of APC positive cells (mature oligodendrocytes) in the WMI group returned to the level of the sham group on POD 56 and 84. To further ask whether myelin sheath generation returned to normal, immunofluorescence staining and western

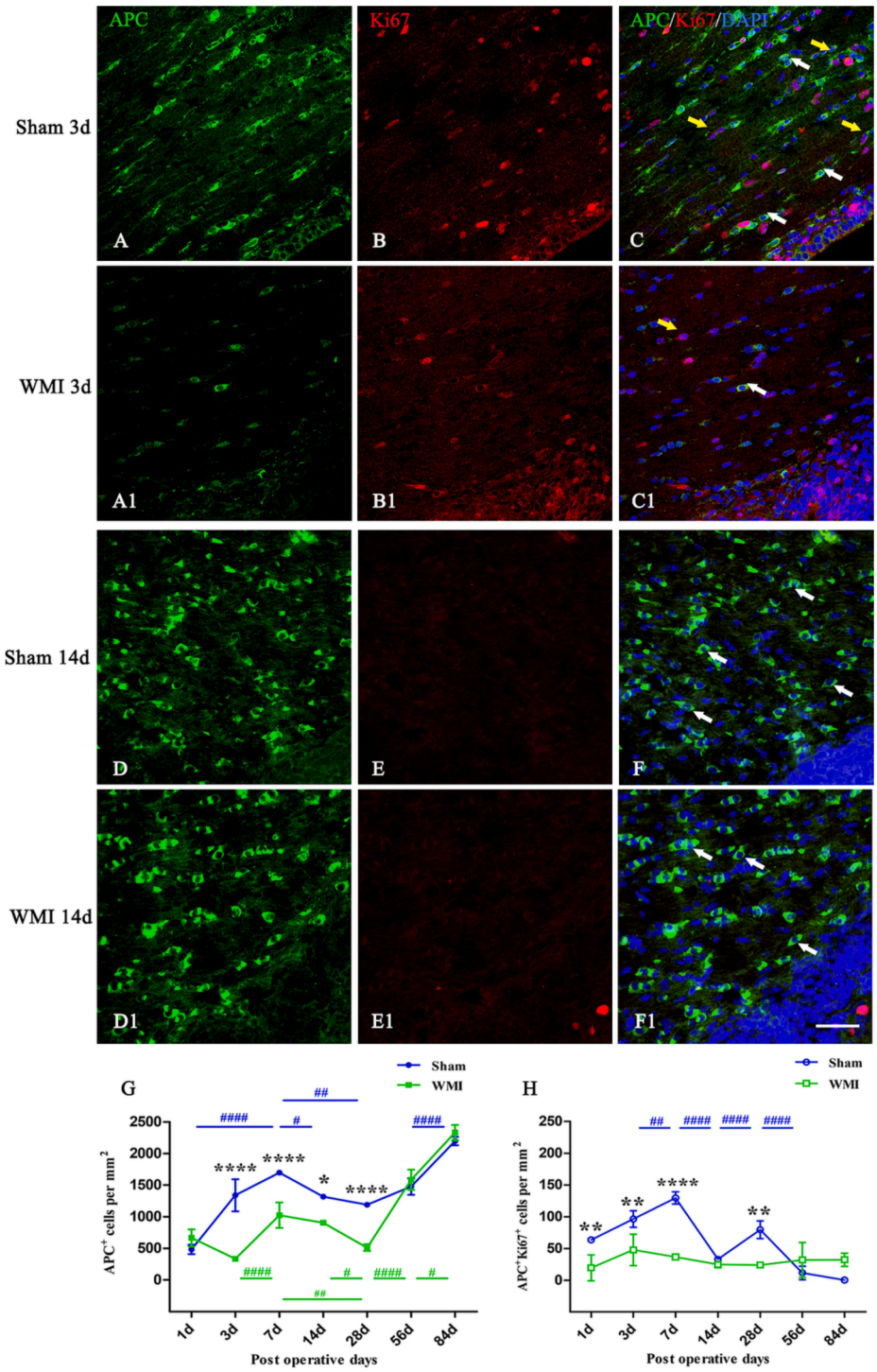

Fig. 7. The effect of hypoxia–ischemia on the total number and proliferation of mature oligodendrocytes (OLs) in white matter. **(A-F) and (A1-F1)** Representative images of the immunolabeling for APC (green), Ki67 (red) and DAPI (blue) in the cerebral white matter (corpus callosum [CC]) on postoperative day (POD) 3 and 14. The representative APC/DAPI-positive cells (white arrow) show the mature OLs, the representative APC/Ki67/DAPI-positive cells (yellow arrow) show the proliferation of mature OLs. **(G-H)** The chart of changing trends in the total number of mature OLs and proliferative OPCs in white matter (CC) over time. *Indicates a statistical difference between the sham group and the WMI group at the same postoperative time point ($^{*}p < 0.05$, $^{**}p < 0.01$, $^{****}p < 0.0001$); # indicates that the same group has statistical differences at different postoperative time points ($^{\#}p < 0.05$, $^{\#\#}p < 0.01$, $^{\#\#\#\#}p < 0.0001$). All data represent the mean ± SD, two-way ANOVA with Tukey's multiple comparison test, n = 4 per group. Scale bar, 50 μm. (For interpretation of the references to colour in this figure legend, the reader is referred to the web version of this article.)

blotting were used to detect MBP expression at these two time points. The results showed that the fluorescence intensity of MBP immunopositive substances in the CC of the WMI group was significantly weaker than that of the sham group (Fig. 8A-8D). Western blotting also showed that compared with the sham group, MBP expression in the WMI group was significantly downregulated (Fig. 8E-8F).

4. Discussion

Myelin is a major component of the white matter, and in the central nervous system, mature OLs protrude many processes, contact and wrap neuronal axons with myelin, and subsequently form many helical myelin sheaths(Baumann and Pham-Dinh, 2001). MBP is an important marker of the myelin sheath, and its expression level is directly related to whether OLs have a function to myelination (Buser et al., 2012). To determine whether white matter injury occurred after hypoxia–ischemia in SD rats, we used immunofluorescence staining and western blotting to detect the changes in MBP expression. The results showed that MBP expression was significantly downregulated on POD 14 and 28, suggesting that OL function was impaired and could not differentiate and mature into functional myelin sheath, resulting in WMI, which is consistent with the results of Cai et al (2006). Therefore, this model can

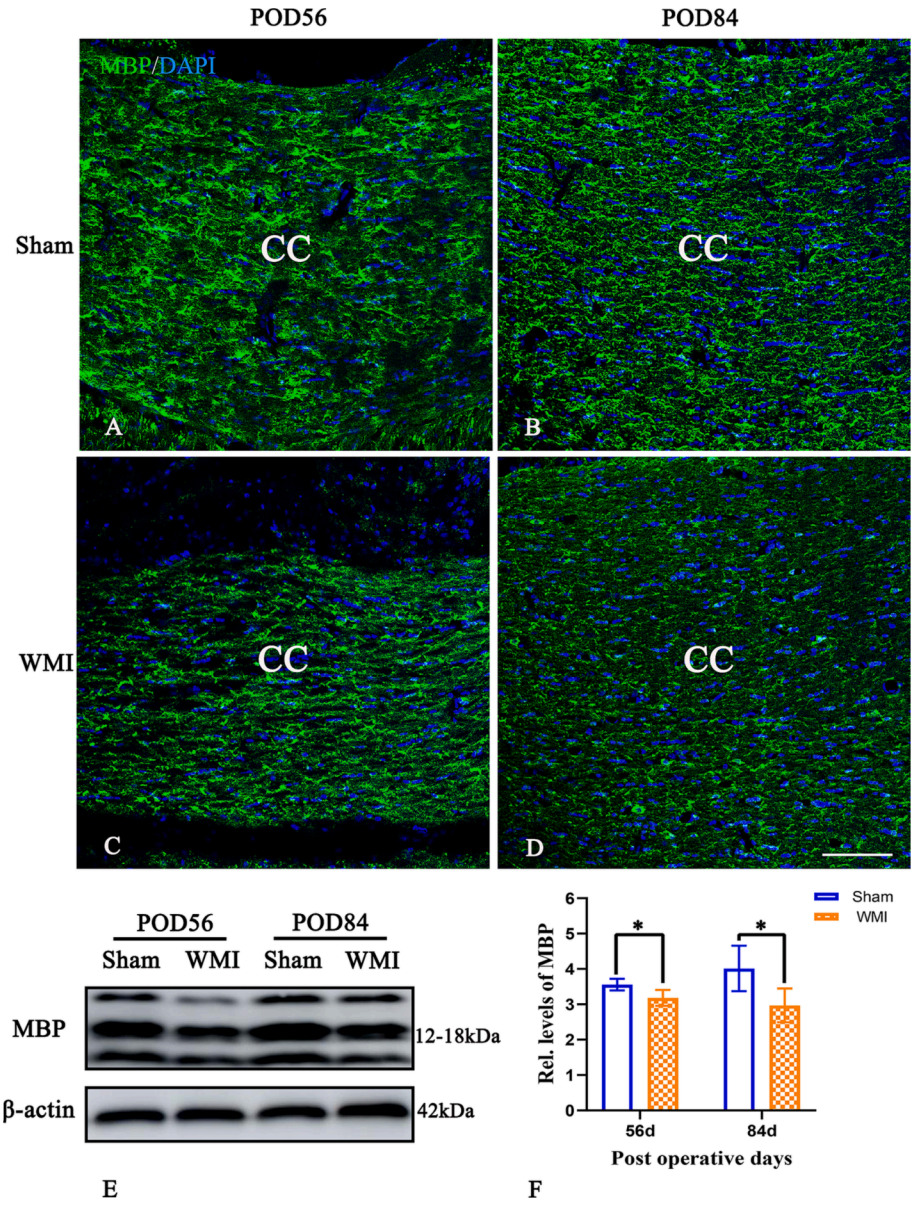

Fig. 8. The effect of hypoxia–ischemia on myelin basic protein (MBP) level in brain on postoperative day (POD) 56 and 84. **(A-D)** Representative images of the immunolabeling for MBP (green) and DAPI (blue) in the cerebral white matter (corpus callosum). Scale bar = 50 μm. **(E-F)** Western blot images show MBP level clearly reduced in WMI group compared with sham group. Detected western blot intensities for MBP were normalized to corresponding β-actin band intensities. All data represent the mean ± SD. *$p < 0.05$, unpaired t test, n = 4 per group. Scale bar, 100 μm. (For interpretation of the references to colour in this figure legend, the reader is referred to the web version of this article.)

be used in subsequent experiments.

OL development can be divided into five main stages: pre-progenitor, progenitor, pre-OLs, pre-myelinating OLs, and myelinating OLs. These have different specific markers at each stage; several transcription factors, olig1/2, NKX2.2, and Sox10, are stably expressed at all stages of OL lineage development. Mature OLs develop from OPCs, which can express PDGFRα (Shaw et al., 2021) and accounts for 5% of the central nervous system of adult rodents. These progenitor cells undergo an immature premyelination stage, and myelin-forming OLs can be identified by expressing myelin-specific proteins, of which MBP and proteolipid protein are major proteins (Pringle et al., 1992). To observe dynamic changes in oligodendrogenesis over time after hypoxia–ischemia, immunofluorescence staining of brain tissues was performed using OL-specific markers combined with cell proliferation markers.

Olig2 and Ki67 immunofluorescence staining were used to observe the overall trend of the OL lineage. The results showed that the number of OL lineages in the sham group first increased (postnatal day [P] 17 peak), then decreased, and finally stabilized. The fastest growth period of OL lineages was observed from POD 3 to 14 (P6-P17), which is consistent with previous research results. Rivers et al. showed that OLs were mainly produced within the first few postnatal weeks and peaked in the second postnatal week (P7-P14) (Rivers et al., 2008). However, the number of OL lineages in the WMI group peaked on POD 3 but was significantly lower than the peak in the sham group, and then remained at the same level, which suggested that OLs death is particularly prominent following hypoxia–ischemia, resulting in a significant decrease in cell number. We counted proliferating OL lineages and found that the change trend of the WMI and sham groups was basically the same over time, and the proliferation peak of OL lineages was concentrated from POD 1 to 14 (P4-P17), which was similar to the results of the study by Levison and Goldman (1993). They discovered that OLs originated from the subventricular zone, and the peak period of OL development was P5–P20. Further analysis of the results of this study showed that the number of proliferating cells in both groups decreased while the total number of cells increased from POD 1 to 3, suggesting that the OL lineage may migrate from other regions to the CC region during this period. On POD 7, the number of proliferating cells in both groups reached the peak, but the total number of OL lineages in the WMI group decreased. The possible reason for this was that hypoxia–ischemia resulted in a significant increase of cell apoptosis,which has been

demonstrated by counting of apoptotic oligodendrocytes. On POD 14, the number of neonatal cells in the sham group decreased significantly, and a decline in the total number of cells was observed. However, the number of neonatal cells decreased, but the total number of cells remained the same in the WMI group, which may be due to the decrease in the number of apoptotic cells or the increase in OLs that migrated from elsewhere.

Previous studies have shown that OLs progenitors migrate from subventricular zone away from these regions and form white matter in the developing brain (Karram et al., 2008; Nishiyama et al., 1996). OL progenitors migrate extensively throughout the central nervous system before eventually differentiating into mature oligodendrocytes (Fard et al., 2017). In our study, immunofluorescence staining was performed with OPC-specific marker PDGFRα and cell proliferation marker Ki67, and it was found that the total number of OPCs and the number of proliferating OPCs in the sham group significantly increased to the peak on POD 7 (P10), decreased on POD 14 (P17), and remained at a low level thereafter, suggesting that OPCs proliferation mainly occurred within 17 days of birth. The results of this study are similar to those of Spitzer et al., who found that the proportion of proliferating OPCs in the white matter decreased significantly after 16 days of birth and remained relatively stable thereafter (Spitzer et al., 2019). The trend in the total number of OPCs and the number of OPCs proliferating over time in the WMI group was consistent with that in the sham group. However, the total number of OPCs and the number of proliferating OPCs in the WMI group were significantly higher than those in the sham group on POD 1, indicating that OPCs had obvious reactive hyperplasia after transient hypoxia–ischemia; therefore, the total number of OPCs was higher than that of the sham group. The total number of OPCs and the number of proliferating OPCs in the WMI group were significantly lower than those in the sham group on POD 3 and 7, suggesting that a longer period of hypoxia–ischemia (POD 3) can inhibit the proliferation of OPCs.

Under normal conditions, OPCs eventually differentiate into mature OLs. By analyzing the changing trend of mature OLs, we found that the proliferation did not show a trend of significant increase or decrease as in the sham group due to hypoxia–ischemia, but remained in a stable state at a low level. The total number of mature OLs in the sham group showed an overall upward trend, while the total number of mature OLs in the WMI group was significantly less than that in the sham group from POD 3 to 28. These evidences implied that a series of oxidative stress reactions caused by hypoxia–ischemia may inhibit the maturation of most OLs. In addition, although OPCs proliferate to varying degrees on POD 14, they may not be able to differentiate into mature myelinated oligodendrocytes (Zhou, et al., 2021), Studies have shown that the main feature of OL failure in the premature brain is the expansion of the preoligodendrocyte population, which is unable to develop further, resulting in a net loss of myelination (Segovia, et al., 2008). However, it should be noted that the total number of mature OLs in the WMI group was not different from that in the sham group from POD 56 to 84. In other words, the level of mature OLs in adult WMI rats was restored to some extent.

MBP expression was determined by immunofluorescence staining and western blotting in order to observe if the recovery of mature OLs increase myelination. The results showed that the expression of MBP in the WMI group was still lower than that in the sham group on POD 56 and 84, indicating that myelin sheath formation was still impaired. These findings implied that OPC deficit may not be the main cause of WMI in late stage. Therapeutic enhancement of myelination is another promising WMI therapeutic strategy. Previous studies have shown that postnatal administration of recombinant human erythropoietin in animal model of WMI could promote myelin formation (Mazur et al., 2010), while administration of erythropoietin in preterm infants did not result in a lower risk of severe neurodevelopmental impairment or death (Juul et al., 2020). And other researchers also found that OLIG1 fails to fully repair injured myelin although it may promote the growth and development of myelin to a certain extent (Cheng, et al., 2015). There are no effective treatment options are clinically available to prevent or cure WMI currently (Motavaf, et al., 2021). Therefore, it is essential to further explore the therapeutic window and pathway following WMI.

In a word, our study indicated that hypoxia–ischemia can affect the endogenous oligodendrogenesis of neonatal rat brain white matter, which may contribute to provide the opportunity to develop new interventions in pre-clinical studies for their promising clinical application. However, the present study also has some limitations. Our findings show the number of mature oligodendrocytes recover to the normal on POD 56 and 84 but the myelination is still blocked. Here we did not provide any mechanistic studies to explain myelin deficiency despite normal cell density. In addition, it would be better using a more elaborated and precise method to study the proliferation of oligodendrocytes rather than only using Ki67.

CRediT authorship contribution statement

Qing Lin: Data curation, Formal analysis, Project administration, Writing – original draft. **Ling Lin:** Formal analysis. **Li Li:** Formal analysis, Writing – original draft. **Yu-fen Zheng:** Formal analysis. **Ding-wang Hu:** Data curation, Writing – review & editing. **Geng Zhang:** Data curation, Project administration, Writing – review & editing.

Declaration of Competing Interest

The authors declare that they have no known competing financial interests or personal relationships that could have appeared to influence the work reported in this paper.

Data availability

The datasets used and/or analyzed during the current study are available from the corresponding author on reasonable request.

Acknowledgement

We thank Dao-shu Luo, Zu-cheng Ye and Feng Wang (School of Basic Medical Sciences of Fujian Medical University) for technical supports. In addition, We would like to thank Shao-wei Lin (School of Public Health of Fujian Medical University) for assistance with statistical analysis.

Funding

This work was supported by Fujian Provincial Natural Science Foundation of China (Grant number: 2017 J01526, 2019 J01292), and Fujian Medical University Qi-hang Fund (Grant number: 2020QH1002).

Ethics approval and consent to participate

Not applicable.

Consent for publication

Not applicable.

References

Almeida, R.G., 2018. The rules of attraction in central nervous system myelination.Front Cell Neurosci 12, 367. https://doi.org/10.3389/fncel.2018.00367.

Back, S.A., 2017. White matter injury in the preterm infant: pathology and mechanisms. Acta Neuropathol 134, 331–349. https://doi.org/10.1007/s00401-017-1718-6.

Back, S.A., Han, B.H., Luo, N.L., Chricton, C.A., Xanthoudakis, S., Tam, J., et al., 2002. Selective vulnerability of late oligodendrocyte progenitors to hypoxia-ischemia. J Neurosci 22, 455–463. https://doi.org/10.1523/JNEUROSCI.22-02-00455.

Baumann, N., Pham-Dinh, D., 2001. Biology of oligodendrocyte and myelin in the mammalian central nervous system. Physiol Rev 81, 871–927. https://doi.org/10.1152/physrev.2001.81.2.871.

Buser, J.R., Maire, J., Riddle, A., Gong, X., Nguyen, T., Nelson, K., et al., 2012. Arrested preoligodendrocyte maturation contributes to myelination failure in premature infants. Ann Neurol 71, 93–109. https://doi.org/10.1002/ana.22627.

Cai, Z., Lin, S., Fan, L.W., Pang, Y., Rhodes, P.G., 2006. Minocycline alleviates hypoxic-ischemic injury to developing oligodendrocytes in the neonatal rat brain. Neuroscience 137, 425–435. https://doi.org/10.1016/j.neuroscience.2005.09.023.

Cai, Q., Ma, T., Tian, Y., Li, C., Li, H., 2018. Catalpol inhibits ischemia-induced premyelinating oligodendrocyte damage through regulation of intercellular calcium homeostasis via Na+/Ca2+ Exchanger 3. Int J Mol Sci 19, 1925. https://doi.org/10.3390/ijms19071925.

Cheng, T.F., Xue, X.D., Fu, J.H., 2015. Effect of OLIG1 on the development of oligodendrocytes and myelination in a neonatal rat PVL model induced by hypoxia-ischemia. Mol Med Rep 11, 2379–2386. https://doi.org/10.3892/mmr.2014.3028.

Derrick, M., Drobyshevsky, A., Ji, X.H., Tan, S., 2007. A model of cerebral palsy from fetal hypoxia-ischemia. Stroke 38, 731–735. https://doi.org/10.1161/01.STR.0000251445.94697.64.

Fancy, S.P., Kotter, M.R., Harrington, E.P., Huang, J.K., Zhao, C., Rowitch, D.H., et al., 2010. Overcoming remyelination failure in multiple sclerosis and other myelin disorders. Exp Neurol 225, 18–23. https://doi.org/10.1016/j.expneurol.2009.12.020.

Fard, M.K., van der Meer, F., Sánchez, P., Cantuti-Castelvetri, L., Mandad, S., Jäkel, S., Fornasiero, E.F., Schmitt, S., Ehrlich, M., Starost, L., Kuhlmann, T., Sergiou, C., Schultz, V., Wrzos, C., Brück, W., Urlaub, H., Dimou, L., Stadelmann, C., Simons, M., 2017. BCAS1 expression defines a population of early myelinating oligodendrocytes in multiple sclerosis lesions. Sci Transl Med 9 (419). https://doi.org/10.1126/scitranslmed.aam7816.

Flygt, J., Djupsjö, A., Lenne, F., Marklund, N., 2013. Myelin loss and oligodendrocyte pathology in white matter tracts following traumatic brain injury in the rat. Eur J Neurosci 38, 2153–2165. https://doi.org/10.1111/ejn.12179.

Hu, D.W., Zhang, G., Lin, L., Yu, X.J., Wang, F., Lin, Q. Dynamic changes of brain iron metabolism in neonatal rats after hypoxia-ischemia. J Stroke Cerebrovasc Dis (2022) 31:106352-59.doi.org/10.1016/j.jstrokecerebrovasdis.2022.106352.

Jablonska, B., Scafidi, J., Aguirre, A., Vaccarino, F., Nguyen, V., Borok, E., et al., 2012. Oligodendrocyte regeneration after neonatal hypoxia requires FoxO1-mediated p27Kip1 expression. J Neurosci 32, 14775–14793. https://doi.org/10.1523/JNEUROSCI.2060-12.2012.

Juul, S.E., Comstock, B.A., Wadhawan, R., Mayock, D.E., Courtney, S.E., Robinson, T., et al., 2020. A randomized trial of erythropoietin for neuroprotection in preterm infants. N. Engl. J. Med 382, 233–243. https://doi.org/10.1056/NEJMoa1907423.

Karram, K., Goebbels, S., Schwab, M., Jennissen, K., Seifert, G., Steinhäuser, C., Nave, K.-A., Trotter, J., 2008. NG2-expressing cells in the nervous system revealed by the NG2-EYFP-knockin mouse. Genesis 46 (12), 743–757.

Levison, S.W., Goldman, J.E., 1993. Both oligodendrocytes and astrocytes develop from progenitors in the subventricular zone of postnatal rat forebrain. Neuron 10, 201–212. https://doi.org/10.1016/0896-6273(93)90311-e.

Lin, Q., Hu, D.-W., Hao, X.-H., Zhang, G., Lin, L., Mangel, S.C., 2023. Effect of Hypoxia-Ischemia on the Expression of Iron-Related Proteins in Neonatal Rat Brains. Neural Plast 2023, 1–11.

Liu, X.B., Shen, Y., Plane, J.M., Deng, W., 2013. Vulnerability of premyelinating oligodendrocytes to white-matter damage in neonatal brain injury. Neurosci Bull 29, 229–238. https://doi.org/10.1007/s12264-013-1311-5.

Marlow, N., Rose, A.S., Rands, C.E., Draper, E.S., 2005. Neuropsychological and educational problems at school age associated with neonatal encephalopathy. Archives of Disease in Childhood - Fetal and Neonatal Edition 90, F380–F387. https://doi.org/10.1136/adc.2004.067520.

Mazur, M., Miller, R.H., Robinson, S., 2010. Postnatal erythropoietin treatment mitigates neural cell loss after systemic prenatal hypoxic-ischemic injury. J. Neurosurg. Pediatr 6, 206–221. https://doi.org/10.3171/2010.5.peds1032.

Nishiyama, A., Lin, X. H., Giese, N., Heldin, C. H., Stallcup, W. B. Co-localization of NG2 proteoglycan and PDGF α-receptor on O2A progenitor cells in the developing rat brain. J Neurosci Res (1996) 43:299–314. doi.org/10.1002/(SICI)1097-4547(19960201)43:3<299::AID-JNR5>3.0.CO;2-E.

Pringle, N.P., Mudhar, H.S., Collarini, E.J., Richardson, W.D., 1992. PDGF receptors in the rat CNS: during late neurogenesis, PDGF alpha-receptor expression appears to be restricted to glial cells of the oligodendrocyte lineage. Development. 115, 535–551. https://doi.org/10.1242/dev.115.2.535.

Rivers, L.E., Young, K.M., Rizzi, M., Jamen, F., Psachoulia, K., Wade, A., et al., 2008. PDGFRA/NG2 glia generate myelinating oligodendrocytes and piriform projection neurons in adult mice. Nat Neurosci 11, 1392–1401. https://doi.org/10.1038/nn.2220.

Santana-Garrido, A., Reyes-Goya, C., Pérez-Camino, M.C., André, H., Mate, A., Vázquez, C.M., 2020. Retinoprotective Effect of Wild Olive (Acebuche) Oil-Enriched Diet against Ocular Oxidative Stress Induced by Arterial Hypertension. Antioxidants 9, 885. https://doi.org/10.3390/antiox9090885.

Segovia, K.N., McClure, M., Moravec, M., Luo, N.L., Wan, Y., Gong, X.i., Riddle, A., Craig, A., Struve, J., Sherman, L.S., Back, S.A., 2008. Arrested oligodendrocyte lineage maturation in chronic perinatal white matter injury. Ann Neurol 63 (4), 520–530.

Shaw, J.C., Crombie, G.K., Palliser, H.K., Hirst, J.J., 2021. Impaired oligodendrocyte development following preterm birth: promoting GABAergic action to improve outcomes. Front Pediatr 9, 618052. https://doi.org/10.3389/fped.2021.618052.

Spitzer, S.O., Sitnikov, S., Kamen, Y., Evans, K.A., Kronenberg-Versteeg, D., Dietmann, S., de Faria, O., Agathou, S., Káradóttir, R.T., 2019. Oligodendrocyte Progenitor Cells Become Regionally Diverse and Heterogeneous with Age. Neuron 101 (3), 459–471.e5.

Volpe, J.J., Kinney, H.C., Jensen, F.E., Rosenberg, P.A., 2011. The developing oligodendrocyte: key cellular target in brain injury in the premature infant. Int J Dev Neurosci 29, 423–440. https://doi.org/10.1016/j.ijdevneu.2011.02.012.

Wang, Z.W., Yang, L.J., Ding, Y.X., Chang, Y.Z., Cui, H., 2016. Insights into the role of iron in immature rat model of hypoxic-ischemic brain injury. Exp Ther Med 12, 1723–1731. https://doi.org/10.3892/etm.2016.3550.

Zhou, N., Wang, L., Fu, P., Cui, Z., Ge, Y., Jiang, F., Liu, J., Ren, C., Luan, Z., Fan, H., Yao, R., 2021. Conditioned medium-preconditioned EPCs enhanced the ability in oligovascular repair in cerebral ischemia neonatal rats. Stem Cell Res Ther 12 (1). https://doi.org/10.1186/s13287-021-02157-4.

Further reading

Franklin, R.J., Blakemore, W.F., 1997. To what extent is oligodendrocyte progenitor migration a limiting factor in the remyelination of multiple sclerosis lesions? Mult Scler 3, 84–87. https://doi.org/10.1177/135245859700300205.

Motavaf, M., Piao, X.H., 2021. Oligodendrocyte Development and Implication in Perinatal White Matter Injury. Front Cell Neurosci 15, 764486. https://doi.org/10.3389/fncel.2021.764486.